Research Paper

Regeneration of CO_2 Physical Solvents at Elevated Pressures in Gas-Liquid Membrane Contactor

Stepan Bazhenov *, Danila Bakhtin, Alexey Volkov

A.V.Topchiev Institute of Petrochemical Synthesis, Russian Academy of Sciences (TIPS RAS), Leninsky prospect 29, 119991, Moscow, Russian Federation

Article info

Keywords

Highlights

- Interaction of PVTMS and physical CO_2 solvents of different classes is studied;
- Asymmetric PVTMS membrane is impermeable toward studied solvents at $\Delta p = 40$ bar;
- CO_2 desorption from water, Genosorb® and [Emim][BF$_4$] in PVTMS-based membrane contactor;
- Best combination of CO_2 flux and pressure difference between gas and liquid phases;
- Membrane structure is stable at transmembrane pressure up to 20 bar within contactor.

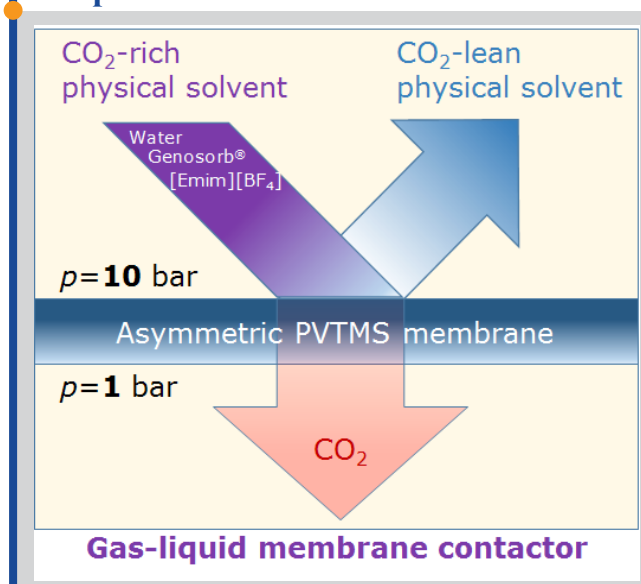## Graphical abstract

Abstract

In the present work, a membrane contactor with asymmetric flat-sheet poly(vinyltrimethylsilane) (PVTMS) membranes was proposed for the CO_2 desorption process from physical solvents at elevated trans-membrane pressures. Different solvents were studied: water, a mixture of polyethylene glycol dimethyl ethers (Genosorb® tradename, Selexol process) and a number of ionic liquids (ILs). The compatibility of PVTMS with physical solvents was evaluated. Thorough sorption and swelling degree tests, FTIR experiments, and solvent permeation study provided insights into PVTMS-solvent interaction and allowed the selection of water, Genosorb® and 1-ethyl-3-methylimidazolium tetrafluoroborate ([Emim][BF$_4$]) as demo solvents for proof-of-concept. CO_2 desorption experiments were successfully realized at elevated trans-membrane pressure (10 bar) and different temperatures (30 and 50ºC). Increasing the temperature from 30 to 50ºC allowed obtaining higher CO_2 desorption flux for all studied solvents. The combination of such parameters as CO_2 flux (up to 4.5 m³ (STP)/(m².h)) and the pressure difference between gas and liquid phases (up to 10 bar) is the best among the available literature data. The detailed investigation of [Emim][BF$_4$] possessing the highest CO_2 flux revealed that an increase of CO_2 content in [Emim][BF$_4$] provided by increasing absorption pressure up to 20 bar resulted in a significant CO_2 desorption flux growth up to 7.5 m³ (STP)/(m².h). Finally, the SEM and EDXS study of membranes after CO_2 desorption tests revealed the deposition of particles containing Na and F elements from ionic liquid [Emim][BF$_4$] on the membrane surface. Nevertheless, the same study proved the stability of the membrane morphology structure at elevated transmembrane pressures even up to 20 bar.

1. Introduction

The integrated process for absorption removal of various components from industrial gas mixtures employing gas-liquid membrane contactors is a dynamically developing area of membrane technology [1, 2]. The principal benefits of membrane contactors are the small size and modularity of the system, since membranes provide high area per unit volume (up to 10000 m²/m³), thus allowing a decrease in the equipment dimensions to more than 60% [3]. Furthermore, a membrane provides independent control of gas and liquid flow rates, whereas the CO_2 absorption selectivity remains high as in conventional absorption processes [4].

Most of the works in the field consider the absorption of carbon dioxide (CO_2) from gaseous streams aimed to decrease anthropogenic CO_2 emission [1]. This technology employs porous hollow fiber membranes made of polypropylene, polytetrafluoroethylene, and polyether ether ketone and has already gained pilot implementation: CO_2 removal was tested for flue gases

[5] and syngas from the pilot pre-combustion plant (Mulgrave, Victoria, Australia) [6]. However, efficient employment of membrane contactors is constrained by a range of pressures close to atmospheric since the operation at elevated pressures might lead to penetration of liquid absorption into membrane pores resulting in a dramatic decline of the mass-transport characteristics [7]. This fact determines the selection of solvent: in most cases, aqueous chemosorbents (aqueous solutions of alkanolamines, ammonia, potassium carbonate, etc.) are employed, since they possess relatively high surface tension and low affinity to polymeric membrane materials [2].

Employment of membrane contactors for CO_2 removal from gaseous mixtures at elevated pressures (1-7 MPa) is feasible when transmembrane pressure is thoroughly controlled [8] or when composite membranes are used: dense highly permeable polymeric layer prevents pore wetting with the solvent [9]. However, industrial purification of gases widely employs physical solvents – liquids in which CO_2 solubility is governed by Henry's law. The sorption capacity of these liquids at elevated partial pressures of CO_2 is higher than that of aqueous-based chemosorbents. Conventional physical solvents are organic liquids with low surface tension: dimethyl ethers of polyethylene glycol (Selexol® process), N-methyl-2-pyrrolidone (Purisol® process), propylene carbonate (Fluor® process), cold methanol (Rectisol® process) [10]. Promising physical solvents are ionic liquids (ILs) – organic salts that are liquids at operating temperature. These liquids provide high CO_2 solubility, almost zero vapor pressure, high thermal stability, relatively low toxicity [11, 12] and even biodegradability [13].

Physical solvents are almost incompatible with modern porous polymeric membranes, as they easily wet the membrane pores [14] and lead to morphological changes of the membrane [15] or its destruction [16]. Theoretical estimations show [17] that it is appropriate to use dense or composite membranes with a thin non-porous layer of highly permeable polymers. Despite the fact that the most permeable disubstituted polyacetylenes are also permeable for physical solvents at elevated pressures [18], the problem can be solved by using a membrane with high CO_2 permeance made of polymeric material having an average CO_2 permeability, which possesses barrier properties towards the penetration of physical solvents.

From this point of view, industrial asymmetric poly(vinyltrimethylsilane) (PVTMS) membranes with a thin dense selective layer are particularly promising. These membranes were originally designed for gas separation processes (hydrogen removal from ammonia syngas, air separation, etc. [19]), however, now they are used in the field of membrane distillation [20]. It should be noted that studies focused on modification of this membrane material to enhance the mechanical properties of fabricated membranes [21, 22] are still in progress.

Industrial asymmetric PVTMS membranes have been successfully employed in membrane contactors for a number of applications: deep removal of oxygen from water [23], air humidity control [24] and olefins removal from mixtures with saturated hydrocarbons [25]. It is especially worth noting that PVTMS membranes have been applied in membrane contactors for CO_2 removal from biogas (biohydrogen, biomethane): they provided efficient carbon dioxide absorption, sterile conditions, and prevention of gas product contamination with liquid solvent [26–29]. As shown by recent studies [30], regeneration of alkanolamine solvents (monoethanolamine – MEA, potassium taurate – PT) at elevated temperatures up to 100°C using PVTMS membranes is also feasible.

Therefore, the present work is focused on the implementation and study of CO_2 removal from physical solvents (solvent regeneration) in membrane contactors based on PVTMS membranes. The physical solvents used were both conventional absorption liquids (water, dimethyl ethers of polyethylene glycol – conventional solvent in Selexol® process) and novel promising solvents — ionic liquids based on imidazolium and phosphonium cations.

2. Experimental

2.1. PVTMS films and asymmetric membranes

The objects of study were industrial samples of asymmetric PVTMS membrane PA-160-C-3.1 with total thickness ~145 μm and dense selective layer thickness 0.25-0.35 μm. The chemical structure of PVTMS is shown in Figure 1, and the cross-section image of the asymmetric membrane is shown in Figure 2.
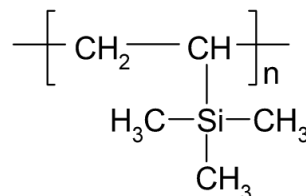

Fig.1. Chemical structure of PVTMS.

For fabrication of dense films, the asymmetric PVTMS membrane samples were dissolved in toluene at room temperature with the following mixing for 24 h. The mixture then was filtered and diluted with toluene until 1 wt% solution was obtained. Dense polymeric films were fabricated by casting the solution onto cellulose film at room temperature. The solutions were covered by Petri dishes to provide slow evaporation of solvent during several days at room temperature. Further drying of the membranes was carried out in a vacuum (residual pressure 0.1 bar) at 40°C to a constant weight. The prepared films were visually transparent, having a thickness of 160±10 μm.

2.2. Physical solvents

The following liquids were applied as physical solvents: distilled water, dimethyl ethers of polyethylene glycols (Genosorb®, Clariant Produkte GmbH), ionic liquids (ILs) purchased from Sigma Aldrich Chemie GmbH – 1-ethyl-3-methylimidazolium dicyanamide ([Emim][DCA], Aldrich #713384), 1-ethyl-3-methylimidazolium tetrafluoroborate ([Emim][BF₄]), trihexyltetradecylphosphonium bromide ([P66614][Br], Aldrich #96662), trihexyltetradecylphosphonium bis(2,4,4-trimethylpentyl)phosphinate ([P66614][Phos], Aldrich # 28612). All the ILs were used without further chemical purification. The only precaution taken was the dry storage under vacuum and elevated temperature (80°C) conditions to avoid any water uptake by the ionic liquid. The water content of used ILs, after drying, was measured by Karl Fischer titration (Metrohm 756 KF Coulometer) and did not exceed 1300 ppm. The chemical structures of used solvents are given in Table 1.
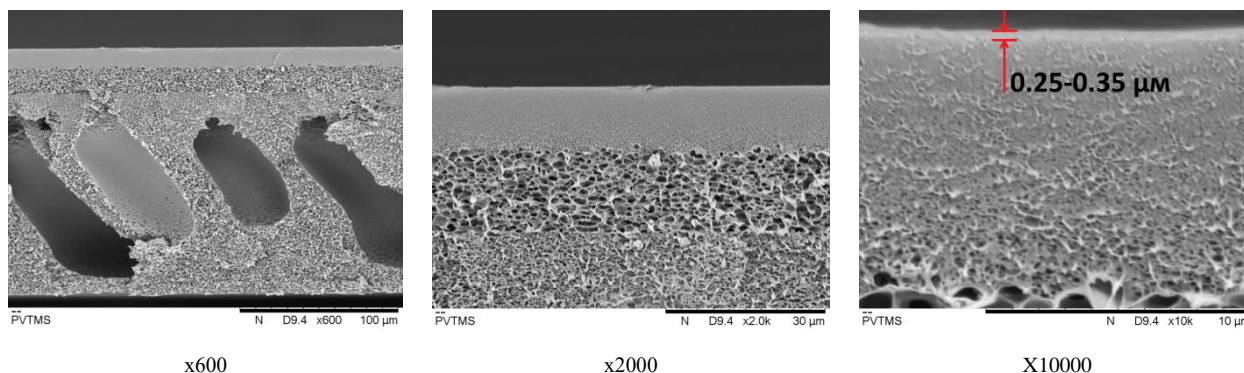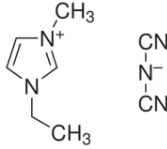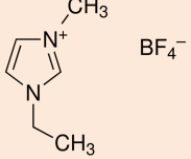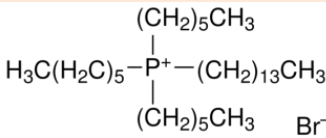

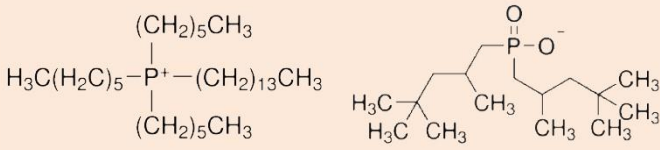|		
x600	x2000	X10000

Fig. 2. Cross-section micrographs of the asymmetric PVTMS membrane at different magnification.

Table 1
The solvents used in the work.

Name	Structure	MW, g/mole
Water	H_2O	18,0
Genosorb®	$H_3CO-(CH_2-CH_2-O)_n-CH_3$ where n = 3-8	280,0
[Emim][DCA]		177,2
[Emim][BF$_4$]	BF_4^-	198,0
[P66614][Br]	$H_3C(H_2C)_5-P^+-(CH_2)_{13}CH_3$ with $(CH_2)_5CH_3$ groups, Br^-	563,8
[P66614][Phos]	$H_3C(H_2C)_5-P^+-(CH_2)_{13}CH_3$ with $(CH_2)_5CH_3$ groups	773,3

2.3. Sorption and swelling degree experiments

The affinity of PVTMS and selected solvents was evaluated through equilibrium values of the liquid sorption in the polymer and swelling degree of the polymer in the liquid. To measure these parameters, the dry square-cut samples of dense films with known size and weight were placed into the studied liquid (3 samples per 1 liquid) and exposed for 6900 hours (9.5 months) at room temperature. After that, the samples were taken from the liquid, and excess of liquid was removed from the film surface with blotting paper prior to size and weight measurements. The sorption value was measured as follows:

$$S = \frac{m - m_0}{m_0} \qquad (1)$$

where m_0 and m (g)– measured values of the sample weight before and after experiments, respectively. The swelling degree of the polymer in the liquid, *SD*, was determined as follows:

$$SD = \frac{d_1 d_2 l - d_{10} d_{20} l_0}{d_{10} d_{20} l_0} \qquad (2)$$

where d_1 and d_2 – length and width of the film, l – the thickness of the film. The subscript "0" means initial film dimensions measured before the experiments.

2.4. Gas and liquid permeation tests

The individual gases (CO_2, N_2, O_2) permeability (*P/l*) through the asymmetric PVTMS membranes was determined with the volumetric technique at temperatures 30 и 50°C [9, 18] as follows:

$$\frac{P}{l} = \frac{V}{St\Delta p} \qquad (3)$$

where V – the volume of gas (m^3 (STP)) passed through the membrane with active area S (m^2) in time t (h) at transmembrane pressure Δp (bar).

The presence or absence of hydrodynamic permeability (permeation) of solvents through asymmetric PVTMS membranes was studied according to the procedure proposed earlier [18]: the membrane sample was placed into a dome-shaped cell, and the upper compartment of the cell above the membrane was partially filled with the studied liquid. Elevated pressure (40 bar) from the solvent side was maintained using pure CO_2. Both the cell and liquid receiver were placed in the heat chamber. The experiments were carried out at 50°C for at least 390 h for each liquid.

2.5. Study of chemical stability of the membranes

The chemical stability of the membranes was studied as follows: the asymmetric PVTMS membrane samples were immersed in the solvents at 50°C for a long time (300 h). Then, the samples were soaked in ethanol for several days and consequently placed in a number of aqueous ethanol solutions with gradually decreasing ethanol concentration. Then, the membranes were placed in distilled water and dried at 40°C. The dried samples were studied via the IR-spectroscopy technique. The spectra were collected at vacuum IR-Fourier spectrometer IFS-Bruker 66/Vs in reflection mode with ZnSe crystal (100 scans, resolution 4 cm^{-1}). Measurements were carried out in the range of 4000-400 cm^{-1} and further processed using OPUS 6.0 software (Bruker). The group of Prof. G.N. Bondarenko carried out iR-analysis at the organometallic catalysis laboratory of TIPS RAS.

2.6. Study of membrane structure and morphology

The structure and morphology of membrane samples were studied with high-resolution scanning electron microscopy (Hitachi Tabletop Microscope TM3030 Plus with a proprietary highly sensitive low-vacuum detector of secondary electrons Hitachi High Technologies America Inc., USA). To obtain the cross-section micrographs, samples were immersed into isopropanol to provide total pore filling and then into liquid nitrogen where they were fractured by a thin razor. The samples were decorated with a thin (~5 nm) layer of gold in a vacuum. In order to determine the elemental

composition of the membrane surface before and after experiments with ionic liquid [Emim][BF₄], the energy dispersive X-Ray spectroscopy (EDXS) analysis was used. The analysis was carried out with a Bruker Silicon Drift Detector coupled with the scanning electron microscope.

2.7. CO₂ desorption from solvents in membrane contactor.

CO_2 desorption from physical solvents was carried out with laboratory setup (see Figure 3) described earlier [9]. Prior to the experiment, absorber *3* was filled with the solvent from tank *1*. Absorber *3* is a high-pressure vessel equipped with a propeller stirrer and temperature controlling system, placed into thermostatic chamber *4*. Carbon dioxide (purity 99.5 vol%) from cylinder *2* was brought into absorber *3* and dissolved in the solvent at constant stirring for at least 4 hours under the following conditions: p_{CO2}= 5, 10 or 20 bar (the pressure was controlled by Bronkhorst® precise controllers); T=30°C. After that, the saturated solvent at the same pressure (5, 10 or 20 bar) was brought into the slit (rectangular) channel of the flat-sheet membrane contactor *6*, which was placed into thermostatic chamber *5*. The channel cross-section was calculated as A_{ch}=Lh=0.04 cm² (channel length L=4 cm, channel height h=0.01 cm,) and the effective membrane area was 16 cm². In the membrane contactor, carbon dioxide was desorbed from the solvent and penetrated through the membrane into the gas compartment of the membrane contactor at atmospheric pressure (no sweep gas or vacuum was applied).

The desorption temperature was 30°C or 50 °C. Desorbed carbon dioxide was removed from the setup and CO_2 flux was measured by an electronic soap film flowmeter "Potok" (OOO "Monitoring") *9*. The flow velocity of saturated solvent through the contactor was controlled by precise valve *11* at the output of the contactor. The solvent flux through the contactor was estimated by a weight method based on the weight of the degassed solvent receiver (*10*), taking into account the solvent density. Liquid penetration into the gas compartment of the membrane contactor was determined visually using the cold trap *7*.

3. Results and discussion

3.1. Gas permeance of the membranes

Gas permeance is a key characteristic of membranes with a dense selective layer. This parameter has to have maximum value in order to minimize the membrane contribution into overall mass transport resistance within the process. Gas transport properties of the asymmetric PVTMS membranes are given in Table 2.

The results show that the membranes have high gas permeance values for all the gases studied (O₂, N₂, CO₂). CO_2 permeance is varied within the range

of 520 – 610 GPU. This value is comparable to that for composite membranes with a thin dense layer (~ 600 GPU [9]) as well as for porous membranes (~ 1000 GPU [31]), which were used in gas-liquid membrane contactors for CO_2 removal. The temperature increase leads to a moderate increase in gas permeance of the membranes, which indicates the stability of their gas transport properties within the range of temperatures specific to physical solvent processes. It should be noted that the results are in good agreement with the data published earlier (see, e.g., [32]). The evaluation of ideal gas selectivity (α) for gas pairs O₂/N₂ and CO₂/N₂ indicates that gas transport in the membrane selective layer is governed by a solution-diffusion mechanism (α > 1). This, in turn, shows that the selective layer does not contain any micro defects or cavities, which is critically important to prevent penetration of physical solvents at elevated pressures within the membrane contactor.

3.2. Interaction between the polymer and physical solvents

The interaction between PVTMS and physical solvents was evaluated by means of measuring equilibrium values of liquid sorption in the polymer and the polymer swelling degree after long-term contact (6900 hours). A comparison of results with the physical properties of the solvents studied (see Table 3) revealed that there is no correlation between viscosity and S/SD values — the results are comparable for both water and [P66614][Phos], viscosities of which differ by three orders of magnitude. On the other hand, the correlation with solvent surface tension is evident: in a row «water - [Emim][DCA] - [Emim][BF₄] - Genosorb®» the solvent having lower surface tension better interacts with PVTMS which is indicated by higher S and SD values. A similar correlation was observed for the highly permeable disubstituted polyacetylene poly[1-(trimethylsilyl)-1-propyne] (PTMSP) after interaction studies with binary water-ethanol mixtures, conventional physical solvents [33] and ionic liquids [34]. In contrast to PTMSP [34], phosphonium-based ILs do not obey this regularity: having the lowest surface tension values, [P66614][Br] and [P66614][Phos], however, weakly interact with PVTMS. Relatively low S and SD values (lower than those for Genosorb® solvent) are supposed to be related to steric hindrance in penetration of the ILs into the PVTMS matrix, polymeric chains of which are relatively rigid. The size of the free volume element in PVTMS is approx. 6–7 Å (120–200 Å³) [19], while the simplest estimations of molar volume of [P66614][Br] and [P66614][Phos] (considering the IL molecules to be spherical) show that their molecular size is ~ 12 Å and ~ 14 Å, which is larger than the PVTMS free volume elements.

Generally, the sorption and swelling degree data for PVTMS show that all the solvents studied relatively weakly interact with the polymer. The only exception is Genosorb®, but its sorption (0.09 g/g) and PVTMS swelling degree (11.9%) values are also low, being 5-10 times lower than those for PTMSP — 1.22 g/g and 59%, respectively [18].
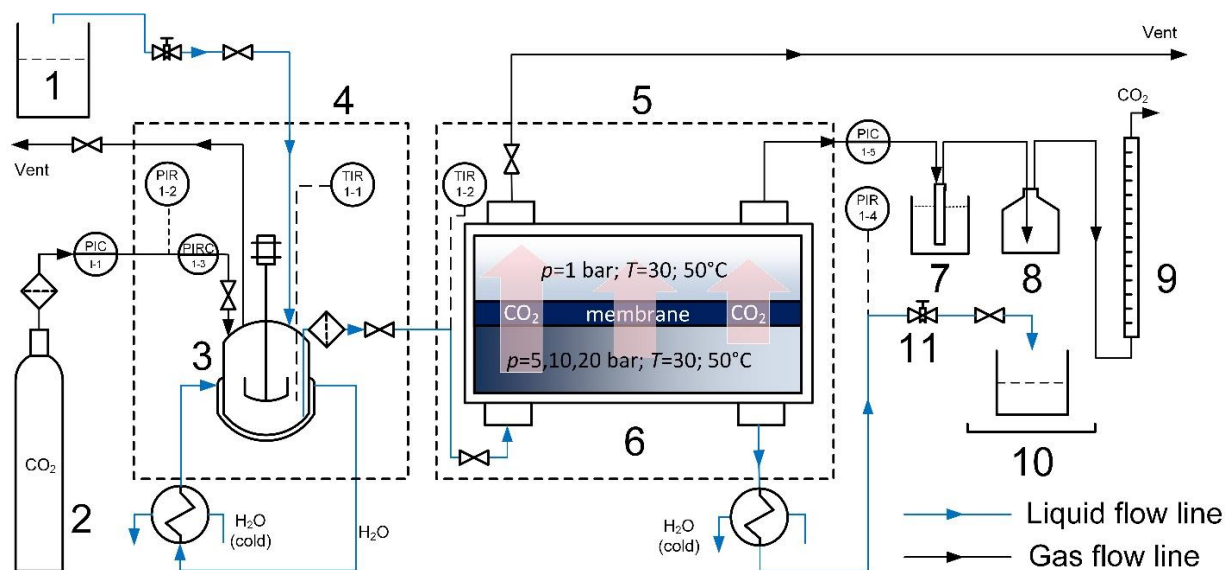

Fig. 3. Membrane gas desorption setup: *1* – initial solvent tank; *2* – CO₂ cylinder; *3* – absorber; *4, 5* – thermostatic chambers; *6* – flat-sheet gas-liquid membrane contactor; *7* – cold trap; *8* – buffer tank; *9* – electronic soap film flowmeter; *10* – degassed solvent receiver with electronic scales, *11* – precise regulation valve.

Table 2
Gas transport properties of PVTMS.

Measurement temperature	P/l (N_2), GPU*	P/l (O_2), GPU	P/l (CO_2), GPU	α(O_2/N_2)	α(CO_2/N_2)
30 °C	48	174	520	3,6	10,8
50 °C	59	212	610	3,6	10,4

*1 GPU = 10^{-6} cm^3 (STP)/(cm^2·s·cm Hg)

Table 3
Interaction between physical solvents and PVTMS: sorption [g/g], swelling degree [%]) at 25 ± 3 °C. The surface tensions, viscosities of liquids and Henry's law constants for CO_2 solubility are also presented.

Physical solvent	Sorption S, g/g	Swelling degree SD, %	Solvent surface tension (25°C, 1 bar), mN/m	Solvent viscosity (25°C, 1 bar), mPa·s	Henry's law constant for CO_2 solubility (H_{12}) at 40°C, MPa
Water	<0.01	<0.1	71.9[35]	0.9[35]	230.94[36]
Genosorb®	0.09	11.9	35.6[37]	7.3[37]	4.70[38]
[Emim][DCA]	0.01	3.3	60.3[39]	14.5[39]	9.59[40]
[Emim][BF₄]	0.01	3.6	54.0[39]	36.9[39]	3.05[41]
[P66614][Br]	0.02	5.9	29.3[39]	2988[39]	6.58[42]
[P66614][Phos]	<0.01	3.6	28.2[39]	1402[39]	0.71[42]

3.3. Determination of hydrodynamic permeability of the membranes and selection of solvents for the CO_2 desorption process

The obtained S and SD data allowed us to suggest that the asymmetric PVTMS membranes are impermeable barriers towards the physical solvents studied. This is highly important because the key requirement in dense membranes for gas-liquid membrane contactors is their ability to exhibit barrier properties towards the solvent permeation. When the liquid penetrates through the membrane into the gas compartment of the membrane contactor, the separated phases mix with each other, and the overall efficiency of the system drops drastically.

To determine the hydrodynamic permeability of the membranes, long-term experiments were carried out at transmembrane pressure of 40 bar and temperature of 50°C. The results showed that neither of the solvents, including Genosorb®, penetrates through the asymmetric PVTMS membranes at given conditions for at least 390 h. Therefore, all the solvents studied can be employed in the CO_2 desorption process.

For further experiments, we have chosen water, Genosorb® and [Emim][BF₄] as representatives of three different classes of compounds. The choice of [Emim][BF₄] from the four ILs was based on CO_2 solubility values. A comparison between Henry's law constants (see Table 3) shows that CO_2 is highly soluble in [Emim][BF₄] (Henry's law constant is one of the lowest — 3.05 MPa). The [P66614][Phos] seems to be even a more promising solvent, as it has Henry's law constant of 0.71 MPa. However, preliminary experiments showed that [P66614][Phos] cannot be employed in the real process since its viscosity is too high (40 times higher than that of [Emim][BF₄] – see Table 3).

3.4. Chemical stability in the physical solvents

One of the key requirements to membranes is their chemical stability in the chosen physical solvents, since they are aggressive chemical agents at elevated temperatures during the long-term process.

The asymmetric PVTMS membrane samples were immersed in sealed vessels containing water, Genosorb® and [Emim][BF₄]. The vessels were placed into a heat chamber and exposed for 300 h at 50°C. Then the membranes were removed from the vessels and cleaned with blotting paper. Visual inspection showed that no change occurred in the membrane color and morphology. Also, no decline in size and mass of the specimens was observed, which indicates that PVTMS does not dissolve in the solvents chosen.

Chemical stability of the membranes was confirmed by IR spectroscopy analysis. Stability of PVTMS in water and aqueous amine solutions at elevated temperatures (up to 100°C) was proven in [30]. In the present work, we studied IR spectra of the PVTMS membranes after exposing them to [Emim][BF₄] (2) and Genosorb® (3) (see Figure 4). For comparison, the initial spectrum of the membrane before experiments (1) is also given. As seen, the spectra are almost identical, which indicates that the chemical structure of

PVTMS did not change (detection limit — $0.5-1.2 \times 10^{-3}$ mol/l). In particular, the spectra do not contain peaks specific to the oxygen-containing groups C–O (1000-1280 cm^{-1}) and C=O (1700-1750 cm^{-1}) [43], which could indicate oxidative degradation of the polymer. Therefore, the asymmetric PVTMS membranes are robust in the used solvents at elevated temperatures. These results combined with the absence of hydrodynamic permeability (paragraph 3.3) allow expecting successful long-term operation of PVTMS in the membrane gas-liquid contactor.

3.5. CO_2 desorption from physical solvents at elevated pressures

The experiments were carried out at transmembrane pressure 10 bar for each of the solvents in order to maintain the equal effect of hydraulic pressure on the membrane. Therefore, the saturation pressure in the absorber (position 3, see Figure 3) did not change and was 10 bar in each experiment. The temperature of solvent saturation with CO_2 was also constant — 30°C. The solvent regeneration process within the membrane contactor was performed at two temperatures — 30°C (as in saturation process) and 50°C. Applying the first temperature value, it was important to confirm that CO_2 desorption from physical solvents is feasible only by means of pressure swing on the other side of the membrane (flash regeneration regime [10]), without increasing the temperature. The second temperature value (50°C) was applied to intensify the desorption process using the thermal regeneration regime which is widely used in the industry [10]. This relatively mild value was chosen to minimize its effect on the PVTMS membrane.

The key parameter of the solvent regeneration process is the volume of desorbed CO_2, penetrating through the active membrane area per time unit (the flux of desorbed CO_2). The relations between this parameter and the linear solvent velocity in a liquid compartment of the membrane contactor have a similar shape for all the solvents studied (see Figure 5) at both values of operating temperature. At higher linear solvent velocity, the flux of desorbed CO_2 increases due to an increase in the number of CO_2 molecules, which were brought with the solvent in the membrane contactor. However, the relation is nonlinear: the linear region extends up to velocities of ~0.01 m/s, while the relation tends to align and achieves a constant value at higher solvent velocities. This behavior seems to be a combination of two effects. The first is the additional diffusional resistance contributed by the membrane. For example, as shown in [44, 45], the transition from porous membranes to those with dense selective layer leads to a significant increase of membrane resistance to CO_2 transport in the membrane contactor. Secondly, the presence of plateau in Figure 5 may be accounted for by a decrease of the solvent residence time in the liquid compartment of the contactor: the CO_2 molecules have less time to diffuse from the bulk of the liquid phase to the surface of the PVTMS membrane at higher solvent linear velocities, which results in decreased overall desorbed CO_2 flux. Our group [9] discovered a similar behavior for alkanolamine chemical solvents. The similar findings were observable in experimental [46] and theoretical [47] works of the other researchers as well.
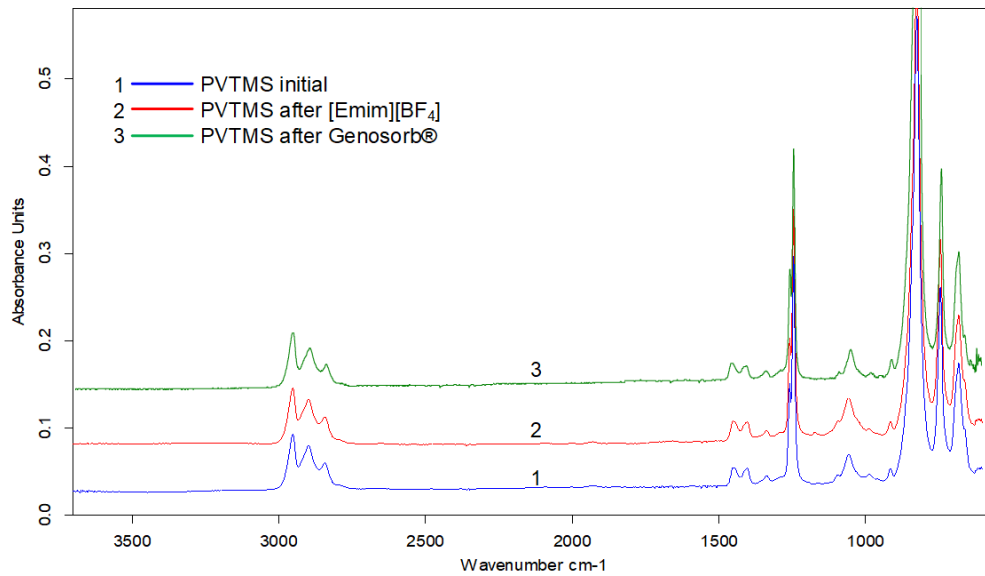
Fig. 4. IR spectra of the asymmetric PVTMS membranes after exposure in Genosorb® and [Emim][BF$_4$] at 50°C for 300 h.
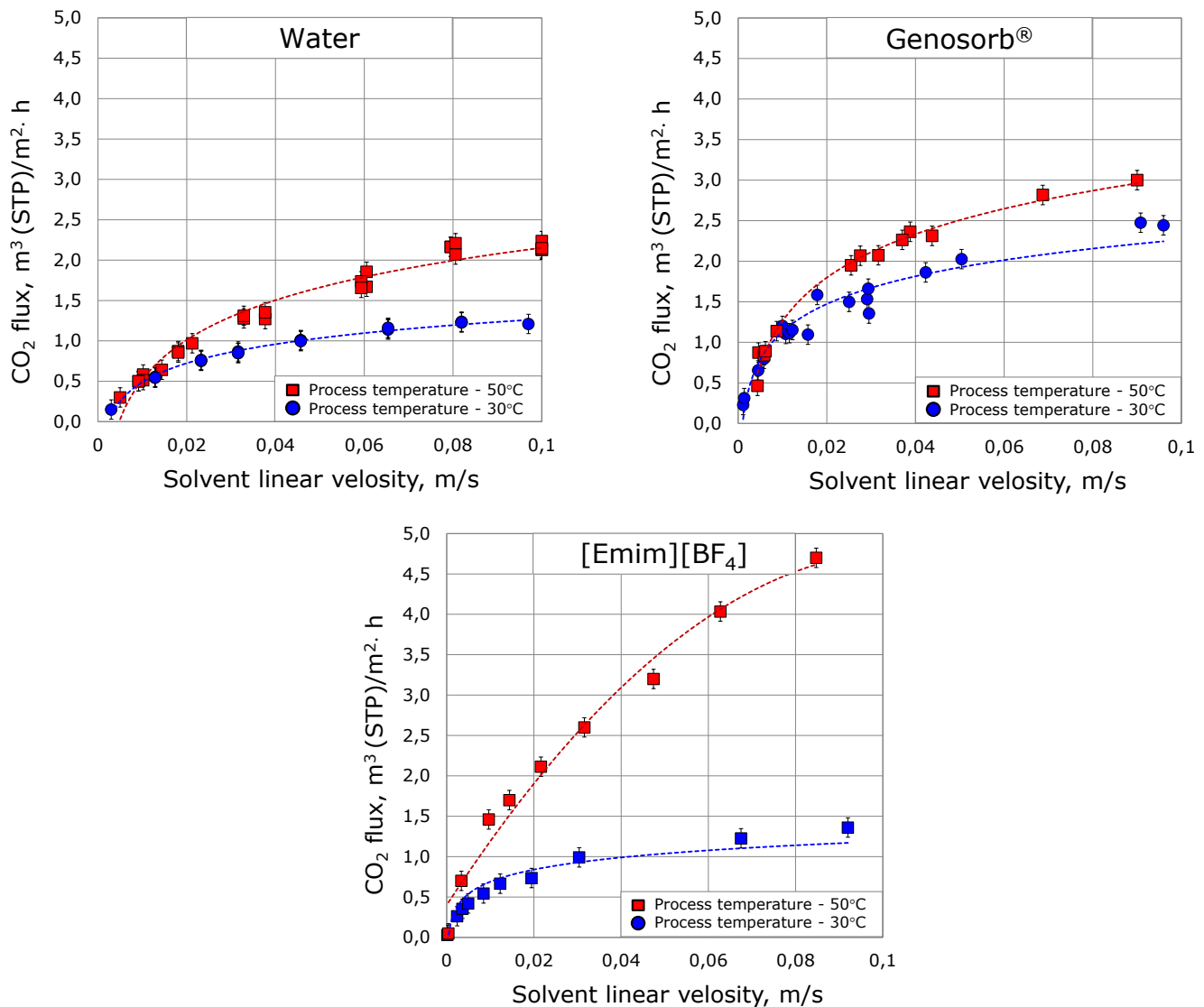

Fig. 5. The effect of solvent linear velocity (water, Genosorb® and [Emim][BF$_4$]) in the liquid compartment of the contactor on the flux of desorbed CO$_2$ at desorption process temperatures 30°C and 50°C. The saturation pressure and liquid pressure in the contactor — 10 bar. The lines through the data points are polynomial fits to guide the eye.

The experimental results (see Figure 5) indicate that the process of CO_2 desorption from the physical solvents can be realized with pressure-swing mode (flash regeneration) exclusively: the flux of desorbed CO_2 reaches significant values at identical temperatures in the absorber and the membrane contactor-desorber (30°C). However, the desorption process can be enhanced with an increase in temperature. We applied higher temperature value, and the desorbed CO_2 flux increased for all the solvents studied (see Figure 5). The result can be explained by a number of factors: 1) CO_2 solubility in the solvents decreases with an increase in liquid temperature, as shown in Table 4, leading to higher driving force of the desorption process; 2) CO_2 permeance of the PVTMS membranes increases at higher temperature, as shown in Table 2.

Detailed analysis of CO_2 desorption from different solvents shows some features. For example, at a temperature of 30°C, the flux of desorbed CO_2 from water is comparable to that for [Emim][BF$_4$], despite the fact that CO_2 solubility in IL is almost two times higher (see Table 4). In contrast, at 50°C, the fluxes differ, being 2-2.5 times higher for [Emim][BF$_4$]. In this case, liquid viscosity seems to have a significant effect, since a decrease in liquid viscosity at higher temperature facilitates the diffusion of CO_2 molecules from the bulk of the liquid phase to the membrane surface. At temperatures from 30 to 50°C, water viscosity decreases by 30% from 0.8 to 0.55 mPa·s [35], while IL viscosity decreases by almost two-fold from 32.3 to 17.3 mPa·s [49].

The data obtained for the Genosorb® solvent are contradictory. CO_2 solubility in Genosorb® is higher than that in water and [Emim][BF$_4$] (see Table 4), while the viscosity of this solvent is relatively low and changes by 39% from 6.35 to 3.89 mPa·s at temperature change (30 to 50°C). However, the fluxes of desorbed CO_2 do not differ significantly (see Figure 5) for different temperatures. This solvent is believed to have a stronger interaction with the PVTMS matrix, which is confirmed by higher S and SD values (see Table 3). In this case, free volume elements of the polymer are partially occupied by bulky oligomeric molecules of Genosorb®, which leads to reduced CO_2 transport efficiency. However, the selected membranes are efficient for CO_2 desorption from Genosorb® at elevated pressures even in such mode.

A very important experimental result is that the physical solvents do not penetrate through the asymmetric PVTMS membranes at a relatively high-pressure difference between gas and liquid phases within the contactor (10 bar). This is confirmed by the absence of any liquid drops in the cold trap 7 of the setup (see Figure 3) during the entire period of research. This phenomenon confirms the conclusions made in paragraph 3.3 and indicates that gas and liquid phases in the membrane contactor do not mix with each other. A wide range of transmembrane pressures (at least up to 10 bar) makes the process very flexible. For example, porous membranes provide efficient CO_2 capture/desorption from physical solvents when the pressure difference between phases is less than 0.5 bar (see data presented in Table 5). Otherwise, the solvent penetrates into the pores of the membrane and drops the process efficiency. Therefore, the transmembrane pressure has to be thoroughly controlled using additional equipment. From this point of view, our results significantly exceed the literature data on CO_2 absorption-desorption by non-aqueous physical solvents at elevated pressures. As shown in Table 5, the PVTMS membranes are both thermally and chemically resistant. Moreover, they provide similar or even higher CO_2 fluxes compared to porous membranes, while the pressure difference between phases within the PVTMS-based contactor is the largest among the known studies.

The results obtained for regeneration of physical solvents with a different chemical nature showed that the highest fluxes of desorbed gas in the membrane contactor are observed for IL [Emim][BF$_4$]. This liquid was used for further detailed research.

3.6. CO_2 desorption from [Emim][BF$_4$].

In the present work, we studied the effect of CO_2 content in IL on the process of CO_2 desorption in the gas-liquid PVTMS-based membrane contactor. Different CO_2 concentration in IL was provided by variation of the saturation pressure in absorber 3 (see Figure 3) at a constant stirring rate. The saturation pressure was 5, 10 and 20 bar, respectively. The saturation temperature was 30°C. Corresponding values of CO_2 solubility at presented pressures and temperature were taken from [41] and are given in Table 6.

Figure 6 The effect of the linear velocity of IL [Emim][BF$_4$] in the liquid compartment of the membrane contactor on the flux of desorbed CO_2 at different CO_2 content in IL (different saturation pressures). Desorption temperatures are 30°C and 50°C. The pressure in the liquid compartment of the contactor — 5, 10 and 20 bar. The lines through the data points are polynomial fits to guide the eye.

The obtained relations between the desorbed CO_2 flux and the linear solvent velocity (see Figure 6) allow concluding that an increase in initial CO_2 content in the IL enhances CO_2 flux. This is a result of the increased driving

force of the membrane desorption process. Elevated temperature favors the process: temperature increasing from 30°C to 50°C results in 3.5 times higher flux of desorbed CO_2 — from 2 to 7 m^3 (STP)/(m^2·h) at a saturation pressure of 20 bar. The same temperature change at a saturation pressure of 5 bar increases the flux two-fold — from 1 to 2 (STP)/(m^2·h). These observations are also in good agreement with the data for CO_2 solubility at an elevated temperature of 50°C, which are given in Table 6.

An important point in the process realization is the fact that changes in CO_2 content in [Emim][BF$_4$] (see Figure 3) are achieved by changing saturation pressure in the absorber, and then IL having the same hydraulic pressure is brought into the liquid compartment of the membrane contactor; i.e., the hydraulic pressure of the liquid phase also changes, being, respectively, 5-20 bar. The experiments showed that an increase of IL hydraulic pressure from 10 bar (studied in paragraph 3.5) to 20 bar (which is, in our case, equal to an increase in transmembrane pressure) does not lead to the appearance of IL in the cold trap 7 (see Figure 3). This indicates that [Emim][BF$_4$] does not penetrate through the PVTMS membranes at elevated pressures up to 20 bar during the CO_2 desorption process. This finding is in good agreement with the barrier properties of the PVTMS membranes studied in paragraph 3.3.

Summarizing the results, one can conclude that ionic liquid [Emim][BF$_4$] seems to be the most promising CO_2 solvent for application in the gas-liquid PVTMS-based membrane contactor since it provides the highest desorbed CO_2 fluxes among the studied physical solvents. Nevertheless, to commercialize the IL solvent for such an application, a number of restrictions (a lack of physicochemical, thermodynamic, lifetime and recyclability data; lack of scale-up, engineering safety, health and environmental studies; high production costs [11]) should be resolved.

3.7. Analysis of the membranes after CO_2 desorption at elevated pressures

As shown earlier in [9], CO_2 desorption at elevated solvent pressures (up to 10 bar) and temperatures (up to 100°C) may lead to morphological changes of the composite membrane and collapse of porous structure of the support, which, in turn, totally blocks the gas transport through the membrane. From this viewpoint, the conditions applied in the present work (transmembrane pressure up to 20 bar, elevated temperature 50°C) constituted a danger to the PVTMS membranes having an asymmetric structure with the macroporous support layer. In order to estimate this impact, the PVTMS membrane sample after the experiments was taken from the contactor followed by removal of IL drops from the membrane surface with blotting paper. Then, the sample was analyzed via the scanning electron microscopy technique combined with energy dispersive X-ray spectroscopy (EDXS).

When comparing the cross-section images of the PVTMS membranes before and after the experiments (see Figure 7), one can conclude that membrane morphology did not change significantly. Moreover, the membrane thickness remained the same. The experiments at elevated liquid pressures do not lead to the collapse of the membrane support structure, thus transport porosity with low mass transfer resistance remains unchanged. EDXS mapping of the images gives evidence that the key elements in both cases are carbon C and silicon Si (as follows from the structure in Figure 1). Nevertheless, as can be seen on the upper part of Figure 7 (d), the membrane surface comprises some inclusions shown by the color blue, which include fluorine F and sodium Na. It should be noted that these inclusions are not presented in the membrane substructure (i.e., do not penetrate into the support through the selective layer).

In order to study the inclusions, SEM images and EDXS mapping of the membrane surface were provided before and after the experiments (see Figure 8). It is obvious that the membrane surface after the experiments comprises individual and agglomerated particles with irregular shape (see Figure 8 (b)). Elemental EDXS mapping (Figure 8 (d)) shows that the particles are mainly constituted by Na and F. Furthermore, mapping of individual elements in Figure 9 shows that the elements are localized in the same particles.
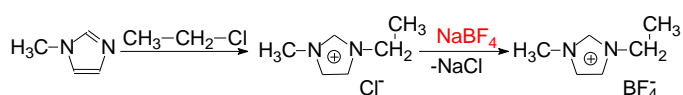
Table 4
The solubility of CO_2 in the solvents.

Solvent	Equilibrium CO_2 solubility, mole/kg		Reference
	P=10 bar, T=30°C	P=10 bar, T=50°C	
Water	0.28	0.19	Calculated from [48]
Genosorb®	1.26	0.78	Calculated from [38]
[Emim][BF$_4$]	0.43	0.28	[41]

Table 5

Implementation of CO_2 absorption-desorption process employing non-aqueous physical solvents in gas-liquid membrane contactors at elevated pressures.

Process	Physical solvent	Membrane type	Pressure conditions	Temperature conditions	Gas type	CO_2 flux, m^3 (STP)/(m²·h)	Remarks	Work
Porous membranes								
CO_2 absorption	Propylene carbonate	Accurel Q3/2 polypropylene hollow fibers.	P=1-20 bar. Pressure difference between gas and liquid phase ≤0.3 bar	T=20-25°C	Pure CO_2 or CO_2/N_2	0.16 – 4.84 (0.002 - 0.06 mole/(m²·s))	Membranes are subjected to morphological changes when used with PC resulted in the wetting of the fiber. The pressure difference between gas and liquid and pressure drops over the fiber length is a critical design parameter provides a non-wetted mode.	[14]
CO_2 absorption	Ionic liquid [Bmim][TCM] - 1-Butyl-3-methylimidazolium tricyanomethanide	Microfiltration tubular glass membrane with hydrophobized surface	P=1-20 bar. Pressure difference between gas and liquid phase <0.5 bar	T = 80°C	CO_2/He - 45/55 vol %	0.008 – 0.02 ((10.4-24.9)×10⁻⁵ mole/(m²·s))	Overall mass transfer coefficients (K_{exp}) and model predictions (K_{ov}) show good agreement at low pressures. Membrane contactor undergoes wetting problems at high pressures (10-20 bar).	[50]
CO_2 absorption	[Bmim][TCM]	PTFE hollow fiber	P=1-20 bar. Pressure difference between gas and liquid phase <0.5 bar	T = 80°C	CO_2/He - 45/55 vol %	0.005 – 0.039 ((0.56-4.86)×10⁻⁴ mole/(m²·s))	The [Bmim][TCM] can gradually attack the membrane in high-pressure conditions and partially dissolve the membrane material after 14 days of experiments.	[16]
Non-porous membranes								
CO_2 absorption	[Bmim][TCM]	Composite type: Teflon AF2400 layer on PP hollow fiber support	P=1-20 bar. Pressure difference between gas and liquid phase <0.5 bar.	T = 80°C	CO_2/He - 45/55 vol %	0.007 – 0.038 ((0.86-4.75)×10⁻⁴ mole/(m²·s))	The CO_2 flux within membrane is reduced at 15% after 14 days of experiments. Composite membranes present good long-term stability.	[16]
CO_2 desorption	DMEPEG	PDMS self-standing	P = 2 bar. Pressure difference between gas and liquid phase - 1 bar.	n/a	Sweeping gas	n/a	Successful CO_2 desorption tests by depressurization under unsteady conditions.	[17]
CO_2 desorption	Genosorb®, Propylene carbonate, N-methylpyrrolidone	Non-porous PTMSP, PTMGP, PMP films (30 μm thickness)	P = 40 bar during long-term solvent permeation tests	T = 100°C	Pure CO_2	n/a	Membranes are chemically stable but permeable to used solvents (possible mixing of gas and liquid phases within contactor).	[18]
CO_2 desorption	Water, Genosorb®, [Emim][BF₄]	PVTMS asymmetric	P = 10 bar. Pressure difference between gas and liquid phase - 10 bar. (P = 40 bar during long-term solvent permeation tests)	T = 30-50°C	Pure CO_2	Up to 3 (Genosorb) Up to 4.5 ([Emim][BF₄])	Successful CO_2 desorption tests at pressure- and temperature-swing modes; no liquid breakthrough through the membrane. Membrane is chemically and thermally stable during long-term tests.	This work

The presence of these elements is not surprising since the most widely used scheme for the synthesis of IL [Emim][BF₄] includes the following chemical reactions (as reported in [51]):

$$H_3C-N \overset{\curvearrowright}{N} \xrightarrow{CH_3-CH_2-Cl} H_3C-\overset{+}{N}\overset{\curvearrowright}{N}-CH_2 \overset{CH_3}{\underset{Cl^-}{}} \xrightarrow[-NaCl]{\color{red}{NaBF_4}} H_3C-\overset{+}{N}\overset{\curvearrowright}{N}-CH_2 \overset{CH_3}{\underset{BF_4^-}{}}$$

In the second stage, the BF_4^- anion is introduced into the IL structure using sodium tetrafluoroborate (highlighted by red color). In our case, residual unreacted $NaBF_4$ seems to form particles on the membrane surface. This fact should be taken into account when applying the membrane contactor with tetrafluoroborate-based ILs during long-term tests, since the deposits of compounds, which were used in the IL synthesis, may deteriorate the process efficiency. However, as stated above, no particles were found in the membrane inner structure (see Figure 7 (d)). This confirms that the selective layer of the asymmetric PVTMS membranes does possess barrier properties towards [Emim][BF₄] in the gas-liquid membrane contactor even at transmembrane pressure of 20 bar.

4. Conclusions

1) For the first time, a study was performed focusing on the interaction between PVTMS and physical solvents of different chemical nature: water, dimethyl ethers of polyethylene glycol (Genosorb®) and ionic liquids based on imidazolium ([Emim][DCA], [Emim][BF₄]) and phosphonium ([P66614][Br], [P66614][Phos]) cations. The long-term (> 6000 h) study of PVTMS sorption and swelling degree confirmed that the polymer has low affinity for all the solvents studied. The asymmetric PVTMS membranes were found to be impermeable for all the liquids at a transmembrane pressure up to 40 bar and temperature of 50°C.

2) The IR spectroscopy analysis proved the chemical stability of the asymmetric PVTMS membranes in the selected physical solvents at elevated temperature (50°C).

3) For the first time, the comparative experiments were performed considering carbon dioxide desorption from the physical solvents of different classes – water, Genosorb® and [Emim][BF₄] – in the gas-liquid membrane contactor with asymmetric PVTMS membranes at a transmembrane pressure difference of 10 bar. The desorption process was shown to be implemented by means of depressurization (pressure-swing mode), exclusively at a constant temperature in the system "absorber – membrane desorber". With a temperature increase from 30°C to 50°C, the process intensifies and the flux of desorbed CO_2 increases. The highest CO_2 fluxes (up to 4.5 m^3 (STP)/(m²·h)) are observed for ionic liquid [Emim][BF₄]. Moreover, this work presents the best combination of pressure difference between phases (10 bar) and the desorbed CO_2 flux among the data available in the literature.

4) The detailed experiments with [Emim][BF₄] showed that the increase in CO_2 concentration in the liquid provided by variation of saturation pressure in the absorber (from 5 to 20 bar) results in the proportional growth of the desorbed CO_2 flux. At a saturation pressure of 20 bar, the switch of desorption temperature to 50°C leads to a higher value of CO_2 flux (up to 7.5 m^3 (STP)/(m²·h)).

5) SEM and EDXS analysis of the PVTMS membrane after the experiments with [Emim][BF₄] showed deposits of irregular-shaped particles and their agglomerates containing Na and F elements on the membrane surface. Nevertheless, this study showed that the membrane inner structure does not include these particles. Furthermore, it was proven that the increased transmembrane pressure (up to 20 bar) in the contactor does not lead to morphological changes of the membrane structure.

Table 6

Equilibrium CO_2 solubility in [Emim][BF₄] (adapted from [41]).

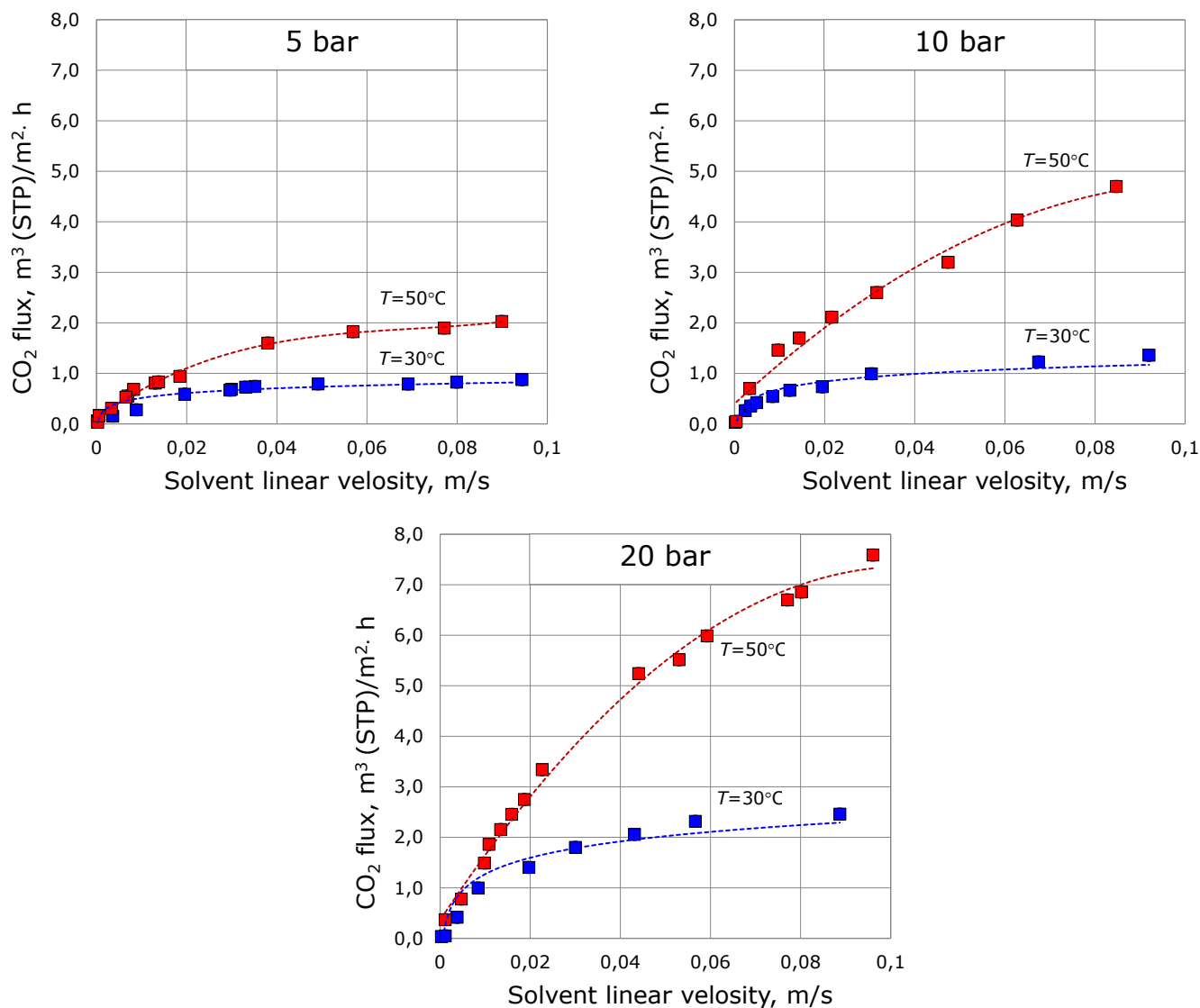| Temperature	CO_2 solubility in [Emim][BF₄], mole CO_2/ kg of [Emim][BF₄]		
	P=5 bar	*P*=10 bar	*P*=20 bar
T=30°C	0.21	0.43	0.86
T=50°C	0.12	0.28	0.59

Fig. 6. The effect of the linear velocity of IL [Emim][BF₄] in the liquid compartment of the membrane contactor on the flux of desorbed CO₂ at the different CO₂ content in IL (different saturation pressures). Desorption temperatures are 30°C and 50°C. The pressure in the liquid compartment of the contactor — 5, 10 and 20 bar. The lines through the data points are polynomial fits to guide the eye.
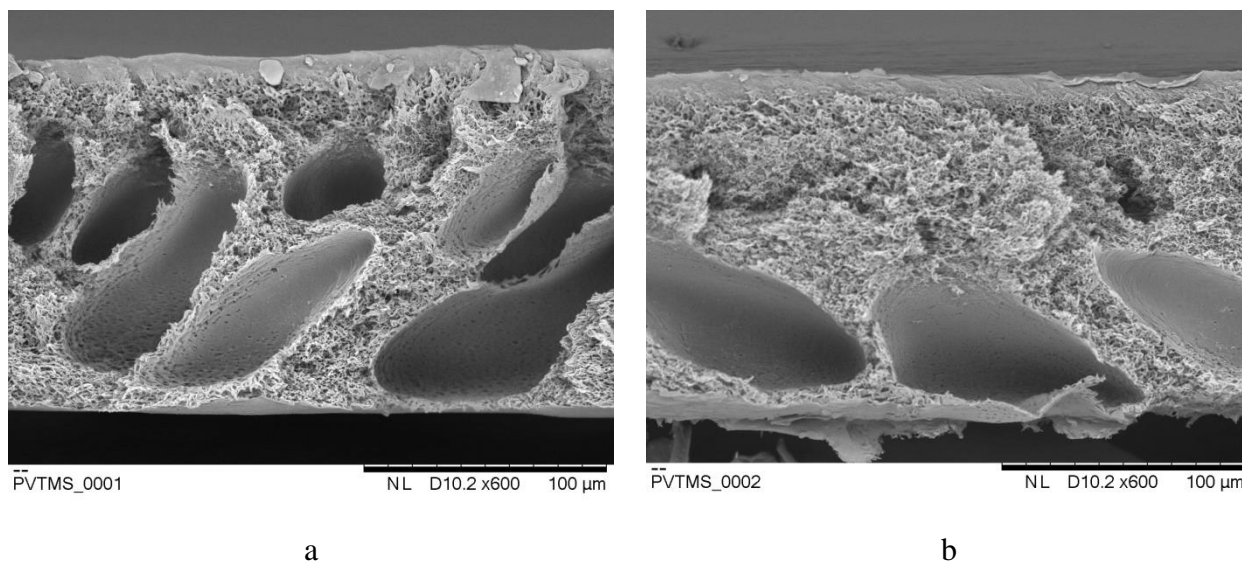

Fig. 7. Cross-section of the asymmetric PVTMS membrane (a) before and (b) after the CO₂ desorption experiments in the gas-liquid membrane contactor at pressures 5-20 bar. Elemental EDXS mapping of the membrane cross-section (c) before and (d) after the desorption experiments.
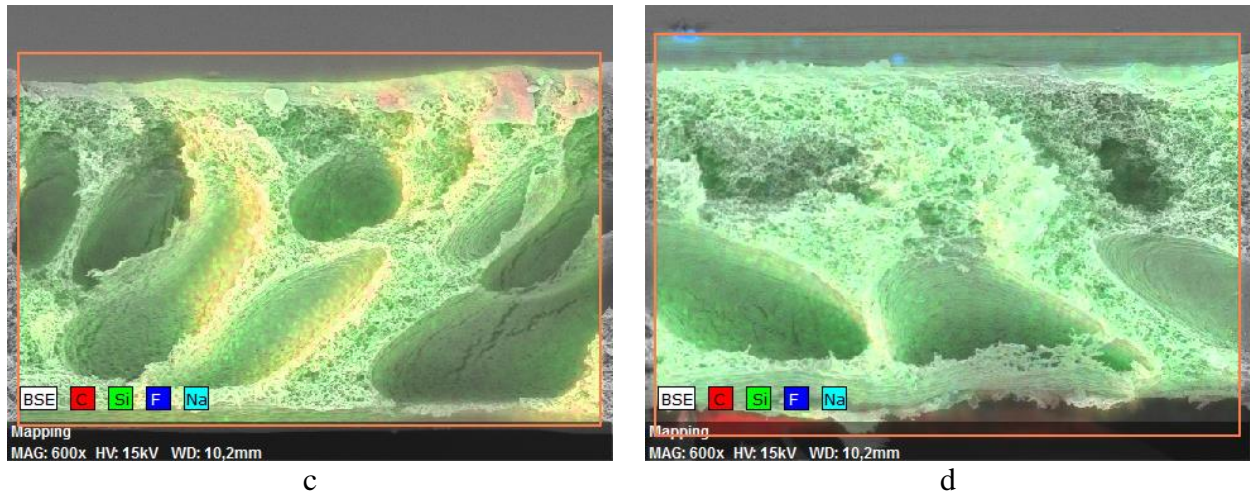
c

d

Fig. 7. Continued.
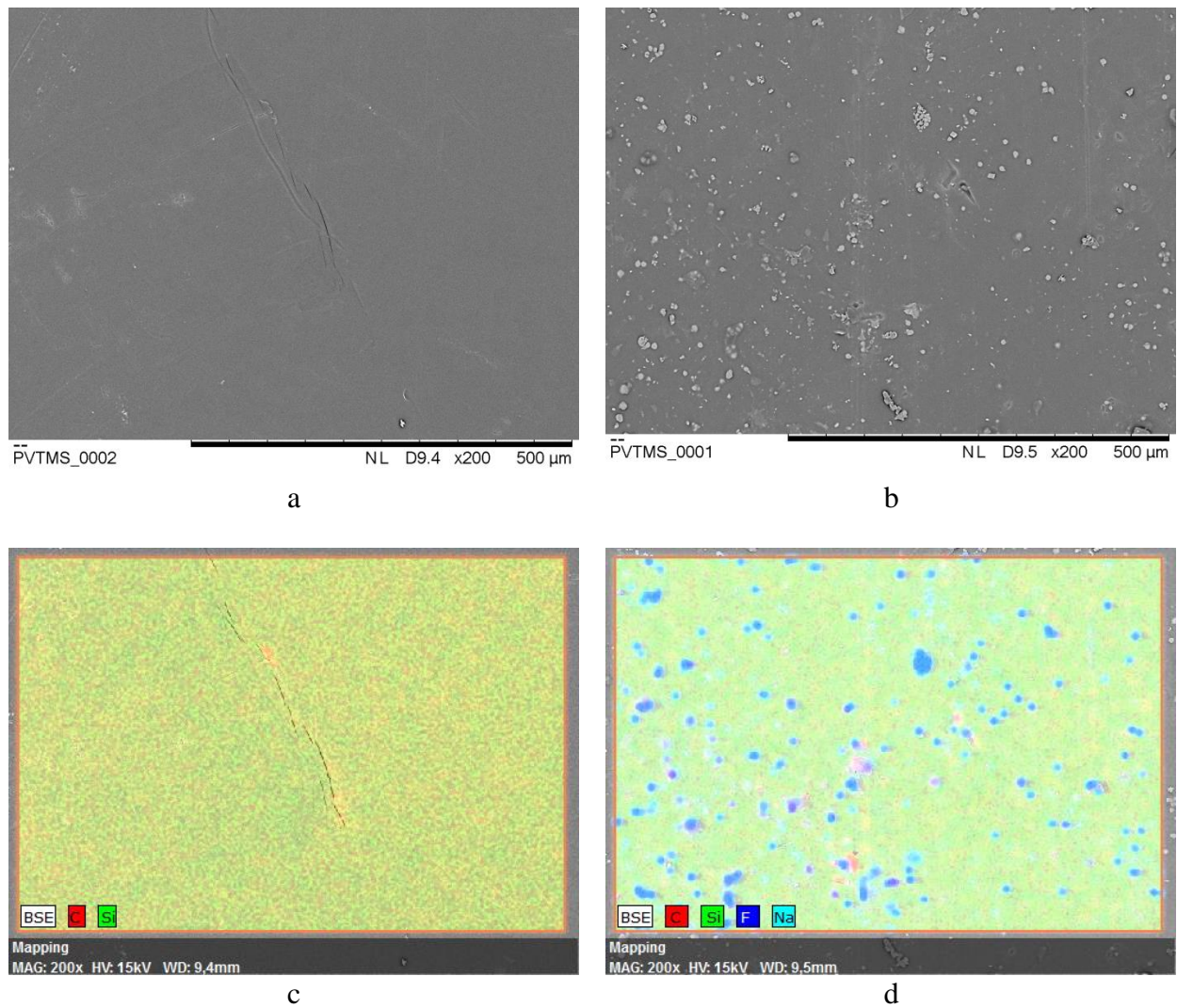

a

b

c

d

Fig. 8. The surface of the selective layer of the asymmetric PVTMS membrane (a) before and (b) after CO_2 desorption experiments in gas-liquid membrane contactor at pressures 5-20 bar. Elemental EDXS mapping of the membrane surface (c) before and (d) after CO_2 desorption experiments.
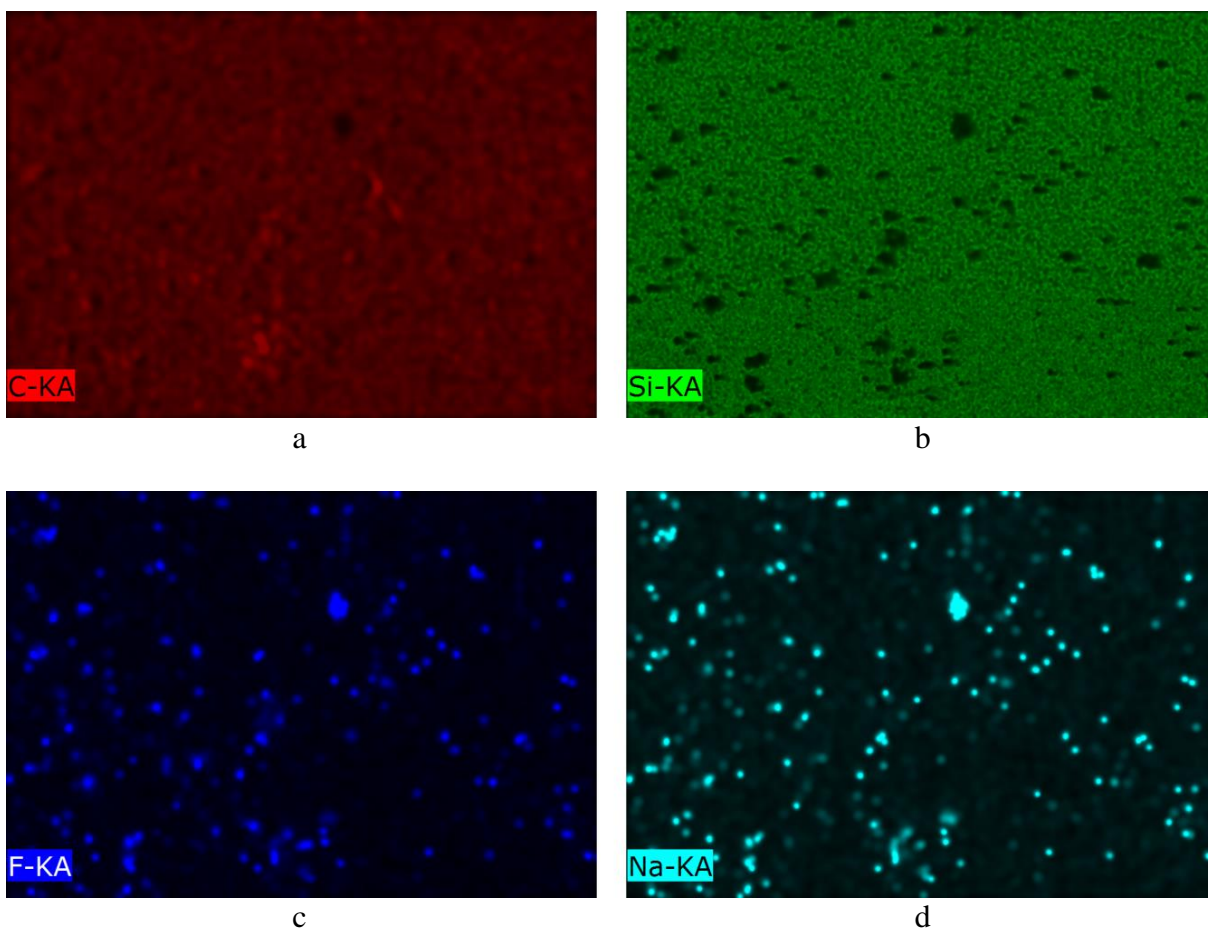
Fig. 9. Elemental EDXS mapping of the asymmetric PVTMS membrane surface after experiments in gas-liquid membrane contactor: a – *C* distribution; b – *Si* distribution; c – *F* distribution; d – *Na* distribution.

References

[1] S. Zhao, P.H. Feron, L. Deng, E. Favre, E. Chabanon, S. Yan, J. Hou, V. Chen, H. Qi, Status and progress of membrane contactors in post-combustion carbon capture: A state-of-the-art review of new developments, J. Membr. Sci. 511 (2016) 180-206.

[2] S.D. Bazhenov, E.S. Lyubimova, Gas–liquid membrane contactors for carbon dioxide capture from gaseous streams, Petrol. Chem. 56 (2016) 889-914.

[3] E. Drioli, A. Criscuoli, E. Curcio, Membrane contactors: fundamentals, applications and potentialities, 1st Ed., Membrane Science and Technology Series 11, Elsevier, Amsterdam, 2006.

[4] A. Ovcharova, V. Vasilevsky, I. Borisov, S. Bazhenov, A. Volkov, A. Bildyukevich, V. Volkov, Polysulfone porous hollow fiber membranes for ethylene-ethane separation in gas-liquid membrane contactor, Sep. Purif. Technol. 183 (2017) 162-172.

[5] S. Li, T. Pyrznski, N. Klinghoffer, T. Tamale, Y. Zhong, J. Aderhold, J. Zhou, H. Meyer, Y. Ding, B. Bikson, Scale-up of PEEK hollow fiber membrane contactor for post-combustion CO₂ capture, J. Membr. Sci., 527 (2017) 92-101.

[6] C.A. Scholes, M. Simioni, A. Qader, G.W. Stevens, S.E. Kentish, Membrane gas–solvent contactor trials of CO₂ absorption from syngas, Chem. Eng. J. 195-196 (2012) 188-197.

[7] S. Mosadegh-Sedghi, D. Rodrigue, J. Brisson, M.C. Iliuta, Wetting phenomenon in membrane contactors–causes and prevention, J. Membr. Sci. 452 (2014) 332-353.

[8] S.A.M. Marzouk, M.H. Al-Marzouqi, M.H. El-Naas, N. Abdullatif, Z.M. Ismail, Removal of carbon dioxide from pressurized CO₂–CH₄ gas mixture using hollow fiber membrane contactors, J. Membr. Sci. 351 (2010) 21-27.

[9] G.A. Dibrov, V.V. Volkov, V.P. Vasilevsky, A.A. Shutova, S.D. Bazhenov, V.S. Khotimsky, A. van de Runstraat, E.L.V. Goetheer, A.V. Volkov, Robust high-permeance PTMSP composite membranes for CO₂ membrane gas desorption at elevated temperatures and pressures, J. Membr. Sci. 470 (2014) 439-450.

[10] A.L. Kohl, R. Nielsen, Gas purification, 5th Ed., Gulf Professional Publishing, Houston, 1997.

[11] M. Ramdin, T.W. de Loos, T.J.H. Vlugt, State-of-the-Art of CO₂ Capture with Ionic Liquids, Ind. Eng. Chem. Res. 51 (2012) 8149-8177.

[12] M. Ramdin, A. Amplianitis, S. Bazhenov, A. Volkov, V. Volkov, T.J.H. Vlugt, T.W. de Loos, Solubility of CO₂ and CH₄ in Ionic Liquids: Ideal CO₂/CH₄ Selectivity, Ind. Eng. Chem. Res. 53 (2014) 15427-15435.

[13] S. Bazhenov, M. Ramdin, A. Volkov, V. Volkov, T.J.H. Vlugt, T.W. de Loos, CO₂ Solubility in Biodegradable Hydroxylammonium-Based Ionic Liquids, J. Chem. Eng. Data 59 (2014) 702-708.

[14] V.Y. Dindore, D.W.F. Brilman, P.H.M. Feron, G.F. Versteeg, CO₂ absorption at elevated pressures using a hollow fiber membrane contactor, J. Membr. Sci. 235 (2004) 99-109.

[15] V.Y. Dindore, D.W.F. Brilman, F.H. Geuzebroek, G.F. Versteeg, Membrane–solvent selection for CO₂ removal using membrane gas–liquid contactors, Sep. Purif. Technol. 40 (2004) 133-145.

[16] Z. Dai, L. Ansaloni, L. Deng, Precombustion CO₂ Capture in Polymeric Hollow Fiber Membrane Contactors Using Ionic Liquids: Porous Membrane versus Nonporous Composite Membrane, Ind. Eng. Chem. Res. 55 (2016) 5983-5992.

[17] E. Chabanon, B. Belaissaoui, E. Favre, Gas–liquid separation processes based on physical solvents: opportunities for membranes, J. Membr. Sci. 459 (2014) 52-61.

[18] A. Trusov, S. Legkov, L.J.P. van den Broeke, E. Goetheer, V. Khotimsky, A. Volkov, Gas/liquid membrane contactors based on disubstituted polyacetylene for CO₂ absorption liquid regeneration at high pressure and temperature, J. Membr. Sci. 383 (2011) 241-249.

[19] Y.P. Yampol'skii, V.V. Volkov, Studies in gas permeability and membrane gas separation in the Soviet Union, J. Membr. Sci. 64 (1991) 191-228.

[20] I.B. Elkina, A.B. Gilman, V.V. Ugrozov, V.V. Volkov, Separation of mineral acid solutions by membrane distillation and thermopervaporation through porous and nonporous membranes, Ind. Eng. Chem. Res. 52 (2013) 8856-8863.

[21] S. Rangou, S. Shishatskiy, V. Filiz, V. Abetz, Poly (vinyl trimethylsilane) and

block copolymers of vinyl trimethylsilane with isoprene: Anionic polymerization, morphology and gas transport properties, Eur. Polym. J. 47 (2011) 723-729.

[22] B.N. Gacal, V. Filiz, S. Shishatskiy, S. Rangou, S. Neumann, V. Abetz, Modification of polyisoprene-block-poly (vinyl trimethylsilane) block copolymers via hydrosilylation and hydrogenation, and their gas transport properties, J. Polym. Sci.: Polym. Phys. 51 (2013) 1252-1261.

[23] D.G. Bessarabov, E.P. Jacobs, R.D. Sanderson, I.N. Beckman, Use of nonporous polymeric flat-sheet gas-separation membranes in a membrane-liquid contactor: experimental studies, J. Membr. Sci. 113 (1996) 275-284.

[24] V.V. Teplyakov, A.Y. Okunev, N.I. Laguntsov, New research and developments in gas/vapor separation by membrane contactor systems, Desalination 200 (2006) 432-434.

[25] D.G. Bessarabov, R.D. Sanderson, E.P. Jacobs, I.N. Beckman, High-efficiency separation of an ethylene/ethane mixture by a large-scale liquid-membrane contactor containing flat-sheet nonporous polymeric gas-separation membranes and a selective flowing-liquid absorbent, Ind. Eng. Chem. Res. 34 (1995) 1769-1778.

[26] M.G. Shalygin, S.M. Abramov, A.I. Netrusov, V.V. Teplyakov, Membrane recovery of hydrogen from gaseous mixtures of biogenic and technogenic origin, Int. J. Hydrog. Energy 40 (2015) 3438-3451.

[27] F. Beggel, I.J. Nowik, M. Modigell, M.G. Shalygin, V.V. Teplyakov, V.B. Zenkevitch, A novel gas purification system for biologically produced gases, J. Clean. Prod. 18 (2010) 43-50.

[28] M.G. Shalygin, D. Roizard, E. Favre, V.V. Teplyakov, CO_2 transfer in an aqueous potassium carbonate liquid membrane module with dense polymeric supporting layers: Influence of concentration, circulation flow rate and temperature, J. Membr. Sci. 318 (2008) 317-326.

[29] M. Modigell, M.V. Schumacher, V. Teplyakov, V.B. Zenkevich, A membrane contactor for efficient CO_2 removal in biohydrogen production, Desalination 224 (2008) 186-190.

[30] A.V. Volkov, S.E. Tsarkov, E.L.V. Goetheer, V.V. Volkov, Amine-based solvents regeneration in gas-liquid membrane contactor based on asymmetric PVTMS, Petrol. Chem. 55 (2015) 716-723.

[31] S. Li, D.J. Rocha, S.J. Zhou, H.S. Meyer, B. Bikson, Y. Ding, Post-combustion CO_2 capture using super-hydrophobic, polyether ether ketone, hollow fiber membrane contactors, J. Membr. Sci. 430 (2013) 79-86.

[32] V.V. Teplyakov, L.G. Gassanova, E.G. Sostina, E.V. Slepova, M. Modigell, A.I. Netrusov, Lab-scale bioreactor integrated with active membrane system for hydrogen production: experience and prospects, Int. J. Hydrog. Energy 27 (2002) 1149-1155.

[33] A. Volkov, A. Yushkin, A. Grekhov, A. Shutova, S. Bazhenov, S. Tsarkov, V. Khotimsky, T.J.H. Vlugt, V. Volkov, Liquid permeation through PTMSP: One polymer for two different membrane applications, J. Membr. Sci. 440 (2013) 98-107.

[34] S. Bazhenov, A. Malakhov, D. Bakhtin, V. Khotimskiy, G. Bondarenko, V. Volkov, M. Ramdin, T.J.H. Vlugt, A. Volkov. CO_2 stripping from ionic liquid at elevated pressures in gas-liquid membrane contactor, Int. J. Greenh. Gas Control 71 (2018) 293-302.

[35] Aspen Properties® version 8.6.

[36] J.J. Carroll, J.D. Slupsky, A.E. Mather, The solubility of carbon dioxide in water at low pressure, J. Phys. Chem. Ref. Data 20 (1991) 1201-1209.

[37] J. Li, M. Mundhwa, A. Henni, Volumetric properties, viscosities, refractive indices, and surface tensions for aqueous Genosorb 1753 solutions, J. Chem. Eng. Data 52 (2007) 955-958.

[38] A.V. Rayer, A. Henni, P. Tontiwachwuthikul, High pressure physical solubility of carbon dioxide (CO_2) in mixed polyethylene glycol dimethyl ethers (Genosorb 1753), Can. J. Chem. Eng. 90 (2012) 576-583.

[39] Ionic Liquids Database - ILThermo (v2.0). http://ilthermo.boulder.nist.gov (accessed 20 February 2018).

[40] D. Camper, C. Becker, C. Koval, R. Noble, Low pressure hydrocarbon solubility in room temperature ionic liquids containing imidazolium rings interpreted using regular solution theory, Ind. Eng. Chem. Res. 44 (2005) 1928-1933.

[41] A.N. Soriano, Jr B.T. Doma, M.H. Li, Solubility of carbon dioxide in 1-ethyl-3-methylimidazolium tetrafluoroborate, J. Chem. Eng. Data 53 (2008) 2550-2555.

[42] M. Ramdin, T.Z. Olasagasti, T.J. Vlugt, T.W. de Loos, High pressure solubility of CO_2 in non-fluorinated phosphonium-based ionic liquids, J. Supercrit. Fluids 82 (2013) 41-49.

[43] V.L. Khodzhaeva, V.G. Zaikin, Fourier transform infrared spectroscopy study of poly (1-trimethylsilyl-1-propyne) aging, J. Appl. Polym. Sci. 103 (2007) 2523-2527.

[44] H.B. Al-Saffar, B. Ozturk, R. Hughes, A comparison of porous and non-porous gas–liquid membrane contactors for gas separation, Chem. Eng. Res. Des. 75 (1997) 685-692.

[45] K. Simons, K. Nijmeijer, M. Wessling, Gas–liquid contactors for CO_2 removal, J. Membr. Sci. 340 (2009) 214-220.

[46] S. Khaisri, P. Tontiwachwuthikul, R. Jiraratananon, CO_2 stripping from monoethanolamine using a membrane contactor, J. Membr. Sci. 376 (2011) 110-118.

[47] N. Ghasem, M. Al-Marzouqi, Modeling and Experimental Study of Carbon Dioxide Absorption in a Flat Sheet Membrane Contactor, J. Membr. Sci. Res. 3 (2017) 57-63.

[48] Z. Duan, R. Sun, An improved model calculating CO_2 solubility in pure water and aqueous NaCl solutions from 273 to 533 K and from 0 to 2000 bar, Chem. Geol. 193 (2003) 257-271.

[49] C.M. Neves, K.A. Kurnia, J.A. Coutinho, I.M. Marrucho, J.N.C. Lopes, M.G. Freire, L.P.N. Rebelo, Systematic study of the thermophysical properties of imidazolium-based ionic liquids with cyano-functionalized anions, The J. Phys. Chem. B 117 (2013) 10271-10283.

[50] Z. Dai, L. Deng, Membrane absorption using ionic liquid for pre-combustion CO_2 capture at elevated pressure and temperature, Int. J. Greenh. Gas Control 54 (2016) 59-69.

[51] G.H. Min, T.E. Yim, H.Y. Lee, D.H. Huh, E.J. Lee, J.Y. Mun, S.M. Oh, Y.G. Kim, Synthesis and properties of ionic liquids: imidazolium tetrafluoroborates with unsaturated side chains, Bull. Korean Chem. Soc. 27(6) (2006) 847-852.